Divergent selection for feed efficiency in pigs altered the duodenum transcriptomic response to feed intake and its DNA methylation profiles

Guillaume Devailly, Katia Feve, Safia Saci, Julien Sarry, Sophie Valière, Jérôme Lluch, Olivier Bouchez, Laure Ravon, Yvon Billon, Hélène Gilbert, et al.

▶ **To cite this version:**

Guillaume Devailly, Katia Feve, Safia Saci, Julien Sarry, Sophie Valière, et al.. Divergent selection for feed efficiency in pigs altered the duodenum transcriptomic response to feed intake and its DNA methylation profiles. Physiological Genomics, 2024, 10.1152/physiolgenomics.00123.2023 . hal-04528954

HAL Id: hal-04528954
https://hal.inrae.fr/hal-04528954v1

Submitted on 29 May 2024

HAL is a multi-disciplinary open access archive for the deposit and dissemination of scientific research documents, whether they are published or not. The documents may come from teaching and research institutions in France or abroad, or from public or private research centers.

L'archive ouverte pluridisciplinaire **HAL**, est destinée au dépôt et à la diffusion de documents scientifiques de niveau recherche, publiés ou non, émanant des établissements d'enseignement et de recherche français ou étrangers, des laboratoires publics ou privés.

RESEARCH ARTICLE

RUNNING HEAD: Transcriptomes and methylomes of the pig's duodenum

Divergent selection for feed efficiency in pigs altered the duodenum transcriptomic response to feed intake and its DNA methylation profiles

Guillaume Devailly[1], Katia Fève[1], Safia Saci[1], Julien Sarry[1], Sophie Valière[2], Jérôme Lluch[2], Olivier Bouchez[2], Laure Ravon[3], Yvon Billon[3], Hélène Gilbert[1], Juliette Riquet[1], Martin Beaumont[1], Julie Demars[1]

[1]GenPhySE, Université de Toulouse, INRAE, ENVT, 31326, Castanet Tolosan, France
[2] INRAE, US 1426, GeT-PlaGe, Genotoul, Castanet-Tolosan, France
[3] Pig phenotyping and Innovative breeding facility, GenESI, UE1372, INRAE, F-17700 Surgères, France

Correspondence: *Guillaume Devailly (guillaume.devailly@inrae.fr).*

ABSTRACT

Feed efficiency is a trait of interest in pigs as it contributes to lowering the ecological and economical costs of pig production. A divergent genetic selection experiment from a Large White pig population was performed for 10 generations, leading to pig lines with relative low- (LRFI) and high- (HRFI) residual feed intake (RFI). Feeding behavior and metabolic differences have been previously reported between the two lines. We hypothesized that part of these differences could be related to differential sensing and absorption of nutrients in the proximal intestine. We investigated the duodenum transcriptome and DNA methylation profiles comparing overnight fasting with ad libitum feeding in LRFI and HRFI pigs (n=24). We identified 1,106 differentially expressed genes between the two lines, notably affecting pathways of the transmembrane transport activity and related to mitosis or chromosome separation. The LRFI line showed a greater transcriptomic response to feed intake than the HRFI line. Feed intake affected genes from both anabolic and catabolic pathways in the pig duodenum, such as rRNA production and autophagy. Several nutrient transporter and tight junction genes were differentially expressed between lines and/or by short term feed intake. We also identified 409 differentially methylated regions in the duodenum mucosa between the two lines, while this epigenetic mark was less affected by feeding. Our findings highlighted that the genetic selection for feed efficiency in pigs changed the transcriptome profiles of the duodenum, and notably its response to feed intake, suggesting key roles for this proximal gut segment in mechanisms underlying feed efficiency.

NEW & NOTEWORTHY

The duodenum is a key organ for the hunger /satiety loop and nutrient sensing. We investigated how the duodenum transcriptome and DNA methylation profiles are affected by feed intakes in pigs. We

observed thousands changes in gene expression levels between overnight-fasted and fed pigs in an high feed efficiency pig lines, but almost none in the related low feed efficiency pig line.

Keywords: DNA methylation; duodenum; feed efficiency; postprandial transcriptome; transcriptomic profiling.

INTRODUCTION

Provide a brief overview of the scope and relevance of the study, especially regarding previous advancements in related fields.

In monogastric livestock, feed efficiency is the ability to convert the greater part of ingested feed into body weight. It is a complex trait with many known influencing factors such as nutrition, metabolism, genetics, microbiome, meteorological conditions, sanitary status, and gut microbiota. Feed efficiency is a trait of great interest for livestock since farming feed cost is a large part of the production costs. Feed also constitutes a large part of the environmental impacts of monogastric farming (1). In addition to research into non-human-edible feed, improvement in the animal feed efficiency will reduce the amount of feed needed to raise livestock, thus contributing to the reduction of its environmental footprint (2–4).

Feed efficiency can be measured as Residual Feed Intake (RFI): the difference between the amount of feed one animal is consuming and the amount predicted for its maintenance and production requirements via multiple regression on several traits (average metabolic body weight, average daily gain, and indicators of body composition). A negative RFI means that the animal is eating less (relatively high efficiency), and a positive RFI means that the animal is eating more (relatively low efficiency) than the population average for their specific growth rate and body composition. RFI is a heritable trait in pigs (5). Differences in blood metabolome and brain, duodenum, liver, and muscle transcriptomes have previously been observed in pigs with contrasted feed efficiency (6–10).

Gilbert et al. created a genetic divergent selection experiment from a Large White pig breed nucleus, resulting in two pig lines of relative low (LRFI) and high (HRFI) residual feed intakes (5). After 10 generations of selection, pigs of the LRFI line eat around 100 grams per day less than pigs from the HRFI to gain a similar amount of body weight, and are thus of greater feed efficiency. The response to selection has led to multiple genetic and genomic changes between the lines (11). A previous transcriptomic study has compared muscle, adipose tissues and liver transcriptome from generation 8 of selection (12), with pathways involved in immune response, response to oxidative stress and protein metabolism differentiating the two lines. These two lines also differ on their blood and muscle metabolism (13, 14)—with a lower insulin level in the blood of LRFI pigs—and in their fecal microbiota (15). The selection has led to distinct feeding behaviors between the lines: pigs from the LRFI line have a lower daily feed intake, wait longer between two visits to the feeder, but eat more per visit, stay longer in the feeder, and eat faster than pigs from the HRFI line (16).

The intestine is known to quickly adapt to various feeding challenges (17). The duodenum is one of the key organs involved in nutrient sensing and satiety regulation, in relation with its proximal position in the gut (18, 19). We hypothesized that divergent selection for feed efficiency might have altered the duodenum physiological response to feed intake. The effect of feeding challenges on intestinal transcriptomes has been investigated by several groups. Zhang et al. reported that pigs submitted to different feeding frequencies, 1, 3 or 5 meals per day, have a different ileal and colonic mucosal transcriptome (20), although they only investigated transcriptomes from overnight fasted pigs. Mazurais et al. studied the impact of a 2-day fasting in the jejunum expression levels of targeted genes in piglets, and noted 146 affected over the 954 studied genes (21). In mice, Yoshioka et al. have investigated the effect of a high-fat and low-fat diet on the duodenal mucosa compared to fasted mice (22). They noted only a modest effect on the transcriptome, but highlighted the downregulation of Slc5a1 after feed intake. *Slc5a1* is the gene encoding for the sodium/glucose cotransporter 1 (SGLT1). It is also documented that the gene *Slc15a1* encoding for the peptide transporter 1 (PEPT1) is downregulated by feed intake in mice (23). More generally, the Solute Carrier (SLC) gene family encodes transmembrane nutrient transporter, and is of great interest to better understand the digestive physiology (24–26).

DNA methylation is an epigenetic mark playing important roles in cellular differentiation and in the regulation of gene expression (27, 28), including in the intestine (29). In mature mammalian tissues, DNA methylation mostly occurs at CpG dinucleotides. Most CpG sites are methylated, except for CpG sites in promoters and enhancers of expressed genes. These unmethylated regions are often relatively enriched in CpG sites compared to the rest of the genome, constituting CpG island in an otherwise CpG depleted genome (30). Promoter DNA methylation is generally negatively correlated with gene expression, while gene body DNA methylation is rather positively correlated with gene expression. Causality links between gene repression and promoter DNA methylation is debated; experimental perturbation of DNA methylation (by knock out, drug, or epigenome editing) often induce transcriptomic changes, but in development and diseases context (such as cancer), gene expression changes mostly occurs before promoter DNA methylation changes (28). DNA methylation is essential for proper intestinal epithelial cell differentiation (31), and DNA methylation profiles change through the intestine's cellular (32) and developmental (33) maturations. In cattle, genomic predictions for feed efficiency are correlated with DNA methylation differences at some imprinted loci (34). A 36h fasting also resulted in changes in DNA methylation in adipose tissues in human (35).

We hypothesized that differences between LRFI and HRFI pigs in the intestinal responses to feed intake might partially explain several of the physiological differences previously reported. We therefore investigated the transcriptomic and DNA methylation profiles of the duodenum mucosa before or after a meal in pigs from the 10th generation of LRFI and HRFI lines, in a total of 24 animals.

MATERIALS AND METHODS

Animal production and sampling

This experimentation was authorised by the French Minister of Higher Education, Research and Innovation under the number APAFIS#21107-2018120415595562 v10, after examinations by the animal experimentation ethic committee number 084.

Animals were raised using standard care in the INRAE pig experimental facility GENESI (36) up until the day before the procedure. Animals were from two French Large White lines of pigs that have been divergently selected on residual feed intakes for 10 generations (5). Pigs were from three litters in each line, and of balanced sexes within litter when possible (one litter was represented by 3 males and one female). At weaning (28 days old on average), animals were split into 2 pens of 12 animals, full-sibs and sexes being equally distributed in the two pens (figure 1A). Pigs were slaughtered on the same day, at the age of 61 days old (min 60 days, max 62 days). The day before sampling, feed access was removed at 5 p.m. in both pens. Animals had free access to water. At 8 a.m. the next day, feed access was introduced back in one pen, but not in the other. Animals were slaughtered by electro-narcosis between 8.50 a.m. and 11.46 a.m., starting with animals left without feed access until 10.10 am where animals with unlimited feed access were also sampled (figure 1B, supplementary table 1). The gastro-intestinal tract was removed, and a 5 cm long section of the duodenum was sampled, opened longitudinally, and the mucosa was collected by scratching the internal duodenal section with a glass microscope slide. Samples were rinsed in PBS, and flash frozen in liquid nitrogen. Samples were preserved at -80°C until extraction.

Sample extraction, library preparation, and sequencing

Frozen duodenum samples were reduced to a fine powder with the mixer-mill MM400 by rapid agitation for 1 minute at 30Hz in a liquid-nitrogen cooled container with stainless steel beads. Fine powder samples were conserved at -80°C until extraction. DNA and RNA were extracted from the powder using NucleoSpin TriPrep mini kit columns (Macherey-Nagel), according to the manufacturer's main instructions but with a few modifications. About 30-50 mg of powder were resuspended in 750 µL of RP1 buffer with 7.5µL of ß-mercaptoethanol then homogenised with the mixer-mill MM400 by rapid agitation for 2x2 minutes at 30Hz with stainless steel beads and incubated 10 minutes at room temperatures. Lysates were loaded into columns in two steps. DNA elution was performed using 65 µL of DNA elute solution. On-column digestion of residual DNA was performed for 30 minutes at room temperature. RNA was eluted using 100 µL of RNase-free water.

RNA-seq libraries were prepared according to Illumina's protocols using the Illumina TruSeq Stranded mRNA sample prep kit to analyse mRNA. Briefly, mRNA were selected using poly-T beads. RNA were reverse transcribed to generate double stranded cDNA, then fragmented, and adaptors were ligated for sequencing. Eleven cycles of PCR were applied to amplify libraries. Library quality was assessed using a Fragment Analyser and libraries were quantified by qPCR using the Kapa Library Quantification Kit. RNA sequencing was performed on an Illumina HiSeq3000 using a paired-end read length of 2 x 150 pb with the Illumina HiSeq3000 Reagent Kits, at the GeT-PlaGe core facility, INRAE Toulouse (37).

Four DNA samples (one female and one male LRFI, one female and one male HRFI) were artificially methylated using the M.Sss1 Enzyme (New England BioLabs) following the manufacturer instruction. DNA libraries (4 fully methylated control, 4 input controls, and 24 samples) were prepared following Bioo scientific's protocol using the Bioo scientific NEXTflex Methyl-seq Library Prep Kit for Illumina Sequencing (part number NOVA-5118-02). Briefly, DNA was fragmented by sonication on a covaris M220 (400-500 bp), size selection was performed using AMPure XP beads and adaptors were ligated to be sequenced. Library preparation failed for one sample (an LRFI fed sample). The 4 fully methylated libraries and the 23 other samples were mixed at equimolarity when possible (62 ng of DNA per sample, otherwise taking a maximal volume of 20 µL resulting in 5-21 ng of DNA for four samples), and a single

methyl-DNA precipitation (MeDP) was performed on 1 µg of the pool using Invitrogen's Methylminer kit following the manufacturer instructions. After additions of the 4 inputs to the pool, 10 cycles of random PCR were performed on the mixed library. Library quality was assessed using an Agilent Fragment Analyser and the pool was quantified by qPCR using the Kapa Library Quantification Kit. MeDP sequencing (MeDP-seq) was performed on two lanes of an Illumina NovaSeq 6000 using a paired-end read length of 2 x 100 bp with the Illumina NovaSeq Reagent Kits S2, at the GeT-PlaGe core facility (37), INRAE Toulouse.

RNA-seq and MeDP-seq libraries were demultiplexed, and the resulting fastq files are available at the ENA database under the id PRJEB46060 / ERP130249.

RNA-seq bioinformatic processing

RNA-seq reads were processed using the nf-core/rnaseq pipeline (38) (version 3.0), using Salmon (39) pseudo-alignment quantifications, Ensembl reference genome Sscrofa11.1, and the corresponding gene annotation file from version 102 of Ensembl (40). Normalised counts were processed using {tximports} (41) to generate transcript per million (TPM) values (supplementary table 2), and gene-length normalised counts (supplementary table 3) were used to carry over differential gene expression analysis with {limma} voom (42), using contrast matrices to test for different factors, and a false discovery rate (FDR) threshold of 5%. The pig line (LRFI or HRFI), condition (fed or fasted) and sex (castrated male or female) were used to build a model matrix. Contrast matrices were constructed to compare the two lines, and to compare the feeding effect within each line. A total of 13,738 genes were analysed, others having less than a total of 8 counts across our dataset. Gene ontology enrichment analysis was performed using {clusterProfiler} (43), using Sus scrofa Gene Ontology. It should be noted that not all genes annotated in the pig genome are associated with a Gene Ontology term, leading to slightly lower gene numbers in gene lists used for the Gene Ontology Analyses. The set of genes used for differential gene expression analysis was used as a reference set. Enriched Gene Ontology were simplified for readability using the *simplify()* function, and simplified enriched ontologies were clustered using the *pairwise_termsim()* function. Heatmaps were generated using {ComplexHeatmap} (44), and upset plots were generated using the {UpSetR} package (45). The list of substrates for each SLC transporter was obtained from the SLC tables at slc.bioparadigms.org (24). The list of tight junction genes was downloaded from the AMIGO gene ontology website (46, 47), using the Gene Ontology term GO:0070160.

MeDP-seq bioinformatic processing

As MeDP-seq data is conceptually similar to ChIP-seq data, MeDP-seq reads were processed using the nf-core/chipseq pipeline (38) version 1.2.1 on Ensembl reference genome Sscrofa11.1 (40). CpG methylation ratios were deduced from MeDP-seq coverages using BayMeth (48) and data from the artificially methylated control samples. Genomic regions with anomalous coverage in input samples were identified using the {greylistchip} bioconductor package (49) version 1.28.1 applied on each of the four input samples separately, and the four greylist regions were merged together. Genomic regions within our greylist were removed from the rest of the analysis.

To define lowly methylated regions (LMRs) we used the following steps: average DNA methylation ratio was computed for each sample in 100 bp windows. We then kept the 100 bp windows for which the DNA methylation ratio was under 40% in at least two samples within LRFI fed, LRFI fasted, HRFI fed, and HRFI fasted pigs. Consecutive 100bp windows were merged, and only genomic regions of 500 bp or

more were kept. Unmethylated regions separated by 300 bp or less were merged. This resulted in the definition of 60,509 LMRs covering 0.03% of the genome (mean size: 1089 bp, median: 700 pb, minimum size: 500 bp, maximum size: 33,500 bp).

MeDP-seq coverage at LMRs was obtained for each sample using {EnrichedHeatmap} normalizeToMatrix function (50). We used {DESeq2}50 to identify LMRs with differential coverage between the two LRFI input control samples and the two HRFI input control samples. This resulted in the identification of 9,572 LMRs with differential coverage between inputs from the two lines at an unadjusted p-value threshold of 5%. These regions were filtered as they might reflect structural genomic differences between the two lines resulting in misestimations of their DNA methylation state by MeDP-seq. Differentially methylated regions (DMRs) between the two lines were identified within the resulting 50,919 lowly methylated regions using {DESeq2} (51) with a linear model taking into account the pig line (LRFI or HRFI) and condition (fed or fasted). Fed/fasted DMRs were called in each pig line independently using the same approach. In addition to an FDR adjusted p-value below 0.05 and after manual visualisations of some regions, we selected only regions with an absolute log2 fold change greater than 1 as differentially methylated regions in an attempt to further reduce false positives. DNA methylation ratio at differentially methylated regions were visualised using {epistack} (52).

Data and script availability

RNA-seq and MeDP-seq reads are available through the ENA database, id PRJEB46060 / ERP130249. Scripts used to process and analyse RNA-seq and MeDP-seq reads are available through a public gitlab repository at the address: forgemia.inra.fr/genepi/analyses/rosepigs. Gene expression counts, lists of differentially expressed genes, sample metadata tables, and DMR positions are available in this repository (forgemia.inra.fr/genepi/analyses/rosepigs/-/tree/master/processed_files). Supplemental material is available at URL: https://entrepot.recherche.data.gouv.fr/dataset.xhtml?persistentId=doi:10.57745/V7FWEH DOI: https://doi.org/10.57745/V7FWEH.

RESULTS

The duodenum transcriptome is different between the high- and low- feed efficiency pig lines

To compare pigs from the 10th generation of selection, 12 animals for each line were taken from 3 litters in the same breeding batch trying to balance sex ratios (figure 1A). After overnight fasting with unrestricted water access, feed was reintroduced to 6 HRFI and 6 LRFI animals in a single pen (balancing litters and sex, figure 1B). Duodenal mucosa samples were then collected, between 2 to 3 hours after feed re-introduction, or between 12 to 14 hours of feed restriction. Duodenal transcriptomes were obtained by RNA-sequencing after poly-A purification, enriching for messenger RNA. We compared 12 LRFI samples (6 fed and 6 fasted) with 12 HRFI samples (6 fed and 6 fasted), and detected 1,106 genes differentially expressed between the LRFI and HRFI lines, independently of the feeding status of the animals (figure 2A, supplementary table 4). In detail, 464 genes were identified as upregulated in the LRFI line, and 642 genes were identified as up-regulated in the HRFI line.

Functional enrichment analysis revealed that genes upregulated in HRFI were notably involved in various aspects of cell division, including spindle checkpoint signalling, chromosome segregation, DNA-templated DNA replication, and immune response (figure 2B). Fewer processes were functionally

enriched in genes upregulated in the LRFI lines (figure 2C), including glycosphingolipid metabolic process and transmembrane transporter activity.

The pig duodenum transcriptome response to feed intake is stronger in LRFI pigs than in HRFI pigs

For each line, we compared duodenal transcriptomes in fasted or fed pigs. We detected 2,222 differentially expressed genes in the LRFI pig line, but only 61 differentially expressed genes in the HRFI line (figure 3, A&B, supplementary table 4), leading to a total of 2,225 genes affected by feed intake in one or both pig lines. Visualisation of expression profiles revealed that in the LRFI line, all 6 fasted pigs were showing stark differences of expression as compared to the 6 fed pigs in the differentially expressed genes, while 3 fasted HRFI pigs and 2 fed HRFI pigs did not have a transcriptomic signature matching the feeding status signature of the LRFI line (figure 3A).

In the LRFI line, the 1,050 genes overexpressed in the fasted state were enriched in GO-BP categories linked to autophagy, cell junction and plasma membrane receptors, Wnt signalling pathway, and protein catabolic processes (figure 3C). The 1,172 genes overexpressed in the fed state in LRFI pigs were enriched in GO-BP categories linked to protein folding, ribosome biogenesis and the sterol biosynthetic process (figure 3D). In the HRFI line, the 41 genes overexpressed in the fasted state were enriched in GO-BP categories linked to ubiquitin ligase complex, and with mitochondrial envelope to a lesser extent (figure 3E). No GO-BP category was detected as enriched in the 20 genes overexpressed in the fed states in HRFI pigs.

Among the genes impacted by the feeding status in one or both lines, 185 genes were also detected as differentially expressed between the two lines (figure 3B). Visual inspection of these genes revealed that they mostly respond to feed intake in the LRFI line and not in the HRFI line, resulting in differences in average expression levels between the lines (figure 3F).

Duodenal expression of nutrient transporter and tight junction genes was altered by the divergent selection on feed efficiency

The transmembrane transporter activity ontology term is overrepresented in genes with higher expression in LRFI than in HRFI (figure 2C). The Solute Carrier (SLC) gene family encodes for transmembrane transporters, including nutrient transporters expressed in the intestinal epithelium (24, 26). We therefore focused our analysis on the expression patterns of the 364 annotated SLC genes in the pig genome in our experimental setup (figure 4A). In the duodenum mucosa, 28 SLC genes are differentially expressed between the LRFI and HRFI lines: 17 are more expressed in the LRFI line, such as the folate transporter *SLC25A32*, 11 are more expressed in the HRFI line such as the glucose and galactose transporter *SLC2A10*. Thirty-five SLC genes are differentially expressed in the duodenum between fasted and fed LRFI pigs between: 18 are more expressed in fasted pigs, such as monosaccharides transporters *SLC5A1* and *SLC2A2* and the aspartate and glutamate transporter *SLC25A13*, 17 are more expressed in fed pigs, such as the glutamate transporter *SLC17A8*. No SLC gene was detected as differentially expressed by feed intake in the duodenum of HRFI pig.

The cell-cell junction organisation ontology term was enriched in genes with higher expression in fasted LRFI pigs than in fed LRFI pigs (figure 3C). We therefore focused our analysis on the expression patterns of the 77 annotated tight junction genes in our experimental setup (figure 4B). In the duodenum mucosa, 5 tight junction genes are differentially expressed between the LRFI and HRFI lines, and all are

more expressed in the LRFI line: Claudin-2 (*CLDN2*), *CLDN4*, *CLDN15*, Partitioning defective 6 homolog beta (PARD6B) and Protein Associated to Tight Junctions / InaD-like protein (*PATJ*). Fifteen tight junction genes are differentially expressed by short term feed intake in the duodenum of LRFI pigs: 12 are more expressed during short term fasting, such as Occludin (*OCLN*), Junctional adhesion molecule A (*F11R*) or *PATJ*, and 3 are more expressed after feed intake: *CLDN5*, *CLDN11* and MICAL-Like 2 (*MICALL2*). No tight junction gene was detected as differentially expressed by feed intake in the duodenum of HRFI pig.

Differences in DNA methylation profiles in the duodenum of LRFI and HRFI pigs

DNA methylation profiles were obtained by MeDP-seq on the same duodenum samples. Although MeDP-seq primarily measures DNA methylation density, we converted it into DNA methylation ratio using fully methylated control samples (see method) (48). For all samples, DNA methylation was lower near the transcription start site (TSS) of expressed genes than at the TSS of un-expressed genes (supplemental figure 1). We detected low DNA methylation regions (LMRs) in each experimental group as putative regulatory regions. Amongst the 50,872 LMRs, 409 were differentially methylated between LRFI and HRFI, 26 were detected as differentially methylated between fasted and fed LRFI pigs, and 3 were detected as differentially methylated between fasted and fed HRFI pigs (figure 5, supplementary table 5, 6, and 7). We did not find global associations between DMRs and differential gene expression, but some overlaps were intriguing. Of the 409 HRFI and LRFI DMRs, 20 were within 20kb of a differentially expressed gene between LRFI and HRFI pigs (supplementary table 8), and the associations between changes in DNA methylation and changes in gene expression were not always in the same direction. Amongst those were *CLDN10* (hypomethylated on the first intron in HRFI, and more expressed in HRFI than in LRFI, figure 6 A&B), *PHGDH* (Phosphoglycerate dehydrogenase, hypomethylated in an internal exon and intron in HRFI, and more expressed in HRFI than in LRFI, figure 6 C&D), *ITLN2* (Intelectin-2, hypomethylated in an internal intron in LRFI, and more expressed in HRFI than in LRFI, figure 6 E&F), *FER* (Proto-oncogene tyrosine-protein kinase, hypomethylated in an internal intron in HRFI, and more expressed in LRFI than in HRFI, figure 6 G&H), and the long non-coding RNA *ENSSSCG00000044004* (hypomethylated at its promoter in HRFI, and more expressed in HRFI than in LRFI, figure 6 I&J). Of the 29 DMRs between fed and fasted pig in one of the lines, 3 were within 20kb of a differentially expressed gene between fasted and fed LRFI pigs (supplementary table 9). Amongst those were *KDSR* (3-dehydrosphinganine reductase, hypomethylated in fed LRFI pigs compared to fasted LRFI pigs, and less expressed in fed LRFI pigs compared to fasted LRFI pigs, figure 6 K&L). *KDSR3* was also less expressed in fed HRFI pigs than in fasted HRFI pigs, but to a lower extent than in LRFI pigs.

DISCUSSION

Explain your interpretation of the data, especially compared with previously published material cited in the References. Significance and limitations may also be present.

Here we demonstrated that the divergent selection on feed efficiency changed the duodenum mucosal transcriptome in pigs, identifying 1,106 genes differentially expressed between the LRFI and HRFI lines. Genes overexpressed in LRFI were enriched in gene ontologies relevant to glycosphingolipid metabolic process, transmembrane transport, and exopeptidase and metallopeptidase activity. These functions do not directly mirror results from the transcriptome of muscle, liver and adipose tissues (12), or in blood, muscle and liver metabolism (13). Therefore, it is likely that genetic differences due to selection have led to differences in gene expression that are distinct between tissues, and are not systemic. Functions enriched in HRFI pigs were overwhelmingly related to mitosis related processes, such as chromosome

separation, DNA replication, and mitosis checkpoint. It is not known if it is due to issues with cell division in the HRFI line that could be frequently failing, or if it simply reflects a higher cell division rate in the duodenum mucosa of HRFI pigs. Histological examination of the duodenum from HRFI and LRFI pigs might be very informative, especially if coupled with measures of cell divisions.

The LRFI line shows a very strong transcriptomic response to feed intake in its duodenum mucosa, with 2,222 differentially expressed genes. Gene expressed after fasting were enriched in catabolic functions and autophagy, while genes expressed after feed intake were more anabolic, which was perhaps to be expected. The large number of differentially expressed genes between fasted and fed LRFI pigs is in contrast to the weak response observed in HRFI pigs, with only 85 differentially expressed genes. It is not known if selection has increased the transcriptomic response in the LRFI line, suppressed the transcriptomic response in the HRFI line, or both at the same time. In mice, only a modest transcriptomic response to feed intake was observed by Yoshioka et al. (22), but it might be due to a relatively poor sensitivity of the SAGE method used in the mice study. We observed that several nutrient transporters had their expression level increased or decreased by feed intake in the LRFI line. We notably confirmed in pigs the previous observation of the downregulation of *Slc5a1* in fasted mice (22). *SLC5A1* encodes for the glucose transporter SGLT1. Different glucose absorption dynamics between LRFI and HRFI lines might lead to different insulinemia, as it has been observed in the same pig lines in earlier generations (13, 14). *SLC4A2* was more expressed in fed than in fasted LRFI pigs. It encodes an anion transporter involved in balancing the cellular pH (53). It was also recently identified in a Epigenome Wide Association Study (EWAS): DNA methylation profiles located at *SLC4A2* correlated with food fussiness in children (54). We did not find any DMR near *SLC4A2* in our dataset. More generally, it is tempting to hypothesise that the lack of transcriptomic response in the duodenum between fasted and fed HRFI pigs might explain some feeding behaviours observed in the HRFI line, for example due to their putative reduced nutrient sensing.

Genes from the cell-cell junction organisation ontology were over-represented in genes more expressed in the fasted condition in the LRFI line. Cell-cell junction, tight junctions in particular, allow the intestine epithelium to act as a barrier between the intestinal lumen and the rest of the organism (55). It may be that LRFI pigs increase the sealing of tight junctions between meals, but HRFI pigs do not. Additional analyses will be required to test this hypothesis, notably histological analyses of the duodenum mucosa or by measuring duodenal permeability. The pathophysiological consequences of this regulation of tight junction induced by genetic selection for feed efficiency should also be investigated, notably in relation with the susceptibility to enteric infections (56, 57).

DNA methylation tends to be absent from active genomic regions (30). Using MeDP-seq, we detected 409 differentially methylated regions between LRFI and HRFI lines using conservative filtering steps. It is likely that a finer DNA methylation measure such as whole genome bisulfite conversion followed by sequencing would have allowed the identification of more differentially methylated regions. Nonetheless, it can be concluded that the selection process for feed efficiency has resulted in distinct duodenal DNA methylation profiles. We only detected 26 and 3 differentially methylated regions between fasted and fed pigs of the LRFI and HRFI line, respectively. Thus, while short term feed intake drastically changes the gene expression profiles of the duodenal mucosa, it barely affects the DNA methylation profiles. Therefore, most—if not all—duodenum gene expression changes between fasted and fed samples were not mediated by DNA methylation changes. It is likely that changes in DNA methylation profiles need more time than changes in gene expression profiles. Nonetheless, it appears

that for DNA methylation profiles as for gene expressions, the LRFI line is more sensitive than the HRFI line to meal intake.

While we could not correlate all the changes in DNA methylation profiles with overall changes in gene expressions, we identify several examples of DMRs located near or within differentially expressed genes (figure 6). This is the case for example for *CLDN10*, involved in tight junctions, *PHDGH*, involved in serine biosynthesis, *ITLN2*, coding for a carbohydrate binding protein, *FER*, a tyrosine kinase regulating cell junctions, *MUC13* (data not shown), a mucin gene, or *KDSR*, involved in the sphingolipid metabolism. The associations between DNA methylation changes and gene expression changes could be either positive or negative, which has been previously reported (58). With this dataset alone, we cannot decipher causalities between the changes in DNA methylations and changes in gene expression levels. Differences between the lines are likely due to genetic effects: selection for feed efficiency have resulted in many genetic differences between the LRFI and HRFI pig lines (11, 59). These genetic differences may alter DNA methylation profiles in cis (i.e. by destroying or creating a transcription factor site) or in trans (i.e. by changing the expression level of a transcription factor or a signaling pathway resulting in downstream DNA methylation changes). We observed no statistically significant difference in gene expression levels between LRFI and HRFI pigs for the DNA methyltransferases *DNMT1*, *DNMT3A*, and *DNMT3B*, nor for the Ten-eleven translocation methylcytosine dioxygenases (TET) *TET1*, *TET2* or *TET3* that are involved in enzymatic DNA demethylation of cytosines (supplemental table 4). We did not detect enough reads assigned to the *DNMT3L* genes to accurately assess its expression levels in our samples. The Ubiquitin-like, containing PHD and RING finger domains, 1 (*UHRF1*) gene was globally more expressed in the HRFI line than in the LRFI line. UHRF1 helps DNMT1 in replicating DNA methylation during DNA replication (60). Further investigations are needed to assess if these changes of UHRF1 expression are of relevance. With our dataset alone, we cannot discriminate if the same genetic differences are involved in changes in DNA methylation and gene expressions, or if the differences we observed are simply coincidental. Genome wide association studies for gene expression levels and DNA methylation levels have the potential to improve our understanding of the difference we describe in the LRFI/HRFI pig lines, but would likely require an order of magnitude more samples to have enough statistical power (61). The long non-coding RNA gene *ENSSSG00000044004* has a DMR right at a lowly methylated region on its promoter, and more DNA methylation is associated with a reduction of its expression. For this case, the correlation between DNA methylation changes and gene expression changes likely reflects causality links. This uncharacterised long non-coding RNA lies between the vasopressin and the oxytocin genes, for which the synteny is conserved in most vertebrates (62).

The pig is thought to be a good model of human digestive physiology (63–65). Compared to rodent models, pigs have a diet, body size, and diurnal rhythm that resemble more the human ones. The dataset produced here might prove useful to better understand the transcriptomic response to feed intake of the human duodenum. Therefore, our dataset is publicly available, at the sequencing read levels, in the form of gene expression tables, and in lists of differentially expressed genes. In addition, better understanding of the biological mechanisms of feed efficiency may contribute to improvements of feed efficiency in pig farming, leading to a more sustainable production.

DATA AVAILABILITY

RNA-seq and MeDP-seq reads are available through the ENA database, id PRJEB46060 / ERP130249. Scripts used to process and analyse RNA-seq and MeDP-seq reads are available through a public gitlab

repository at the address: forgemia.inra.fr/genepi/analyses/rosepigs. Gene expression counts, lists of differentially expressed genes, sample metadata tables, and DMR positions are available in this repository (forgemia.inra.fr/genepi/analyses/rosepigs/-/tree/master/processed_files).

SUPPLEMENTAL MATERIAL

Supplemental material is available at URL: https://entrepot.recherche.data.gouv.fr/dataset.xhtml?persistentId=doi:10.57745/V7FWEH DOI: https://doi.org/10.57745/V7FWEH.

Supplementary table 1: Sample metadata.

Supplementary table 2: Gene expression in Transcript per million, used for visualisations.

Supplementary table 3: Gene expression in pseudo-counts (length-scaled TPM), used differential analysis.

Supplementary table 4: Results of the differential gene expression analysis.

Supplementary table 5: Genomic coordinates of the differentially methylated regions between lines.

Supplementary table 6: Genomic coordinates of the differentially methylated regions between fasted and fed LRFI pigs.

Supplementary table 7: Genomic coordinates of the differentially methylated regions between fasted and fed HRFI pigs.

Supplementary table 8: Line DMRs within 20kb of a differentially expressed gene between LRFI and HRFI pigs.

Supplementary table 9: Fasted vs fed LRFI DMRs within 20kb of a differentially expressed gene between fasted and fed LRFI pigs.

Supplementary figure 1: Low DNA methylation at the promoter of expressed genes. In each MeDP-seq sample, we sorted genes according to expression levels from their corresponding RNA-seq sample, from top (high expression) to bottom (low expression). Genes were binned in three groups of equal size : light green (high expression), dark green (low to no expression), and purple (no expression). For each gene, DNA methylation ratio is represented in the -2.5kb +2.5kb window surrounding their Transcription Start Site (TSS). Bottom panels display the expression values in each bin of genes, as well as their average DNA methylation ratio around TSS. **A.** LRFI samples in the fasted condition. **B.** LRFI samples in the fed condition (one sample failed during library preparation). **C.** HRFI samples in the fasted condition. **D.** HRFI samples in the fed condition.

ACKNOWLEDGMENTS

The authors would like to thank Sophie Leroux and all the GenESI staff for their help with the pig experimentation and sampling (36). We are grateful to the GenoToul bioinformatics platform Toulouse Occitanie (Bioinfo GenoToul (66)) for providing computing and storage resources. GD thanks Sylvain Foissac for his insight in lncRNA gene annotations, and the Bioinfo-fr IRC/Discord community for their

support and insight on Gene Ontology analysis. This work was partially funded by the Animal Genetics department of INRAE.

GRANTS

Agence Nationnale de la Recherche (ANR), grant MicroFeed ANR-16-CE20-0003 (to HG, JR).

DISCLOSURES

The authors declared no conflict of interests.

DISCLAIMERS

None.

AUTHOR CONTRIBUTIONS

Identify which authors participated in the research: Conceived and designed research, performed experiments, analyzed data, interpreted results of experiments, prepared figures, drafted manuscript, edited and revised manuscript, approved final version of manuscript. The information must be the same as in the online submission site.

REFERENCES

1. **Van Zanten HHE**, **Herrero M**, **Van Hal O**, **Röös E**, **Muller A**, **Garnett T**, **Gerber PJ**, **Schader C**, **De Boer IJM**. Defining a land boundary for sustainable livestock consumption. *Glob Change Biol* 24: 4185–4194, 2018. doi: 10.1111/gcb.14321.

2. **Andretta I**, **Hickmann FMW**, **Remus A**, **Franceschi CH**, **Mariani AB**, **Orso C**, **Kipper M**, **Létourneau-Montminy M-P**, **Pomar C**. Environmental Impacts of Pig and Poultry Production: Insights From a Systematic Review. *Front Vet Sci* 8: 750733, 2021. doi: 10.3389/fvets.2021.750733.

3. **Monteiro ANTR**, **Brossard L**, **Gilbert H**, **Dourmad J-Y**. Environmental Impacts and Their Association With Performance and Excretion Traits in Growing Pigs. *Front Vet Sci* 8: 677857, 2021. doi: 10.3389/fvets.2021.677857.

4. **Soleimani T**, **Hermesch S**, **Gilbert H**. Economic and environmental assessments of combined genetics and nutrition optimization strategies to improve the efficiency of sustainable pork production. *J Anim Sci* 99: skab051, 2021. doi: 10.1093/jas/skab051.

5. **Gilbert H**, **Billon Y**, **Brossard L**, **Faure J**, **Gatellier P**, **Gondret F**, **Labussière E**, **Lebret B**, **Lefaucheur L**, **Le Floch N**, **Louveau I**, **Merlot E**, **Meunier-Salaün M-C**, **Montagne L**, **Mormede P**, **Renaudeau D**, **Riquet J**, **Rogel-Gaillard C**, **van Milgen J**, **Vincent A**, **Noblet J**. Review: divergent selection for residual feed intake in the growing pig. *animal* 11: 1427–1439, 2017. doi: 10.1017/S175173111600286X.

6. **Banerjee P**, **Carmelo VAO**, **Kadarmideen HN**. Integrative Analysis of Metabolomic and Transcriptomic Profiles Uncovers Biological Pathways of Feed Efficiency in Pigs. *Metabolites* 10: 275, 2020. doi: 10.3390/metabo10070275.

7. **Ramayo-Caldas Y**, **Ballester M**, **Sánchez JP**, **González-Rodríguez O**, **Revilla M**, **Reyer H**, **Wimmers K**, **Torrallardona D**, **Quintanilla R**. Integrative approach using liver and duodenum RNA-Seq data identifies candidate genes and pathways associated with feed efficiency in pigs. *Sci Rep* 8: 558, 2018. doi: 10.1038/s41598-017-19072-5.

8. **Wang X**, **Kadarmideen HN**. Metabolite Genome-Wide Association Study (mGWAS) and Gene-Metabolite Interaction Network Analysis Reveal Potential Biomarkers for Feed Efficiency in Pigs. *Metabolites* 10: 201, 2020. doi: 10.3390/metabo10050201.

9. **Xu C**, **Wang X**, **Zhuang Z**, **Wu J**, **Zhou S**, **Quan J**, **Ding R**, **Ye Y**, **Peng L**, **Wu Z**, **Zheng E**, **Yang J**. A Transcriptome Analysis Reveals that Hepatic Glycolysis and Lipid Synthesis Are Negatively Associated with Feed Efficiency in DLY Pigs. *Sci Rep* 10: 9874, 2020. doi: 10.1038/s41598-020-66988-6.

10. **Xu C**, **Wang X**, **Zhou S**, **Wu J**, **Geng Q**, **Ruan D**, **Qiu Y**, **Quan J**, **Ding R**, **Cai G**, **Wu Z**, **Zheng E**, **Yang J**. Brain Transcriptome Analysis Reveals Potential Transcription Factors and Biological Pathways Associated with Feed Efficiency in Commercial DLY Pigs. *DNA Cell Biol* 40: 272–282, 2021. doi: 10.1089/dna.2020.6071.

11. **Delpuech E**, **Aliakbari A**, **Labrune Y**, **Fève K**, **Billon Y**, **Gilbert H**, **Riquet J**. Identification of genomic regions affecting production traits in pigs divergently selected for feed efficiency. *Genet Sel Evol GSE* 53: 49, 2021. doi: 10.1186/s12711-021-00642-1.

12. **Gondret F**, **Vincent A**, **Houée-Bigot M**, **Siegel A**, **Lagarrigue S**, **Causeur D**, **Gilbert H**, **Louveau I**. A transcriptome multi-tissue analysis identifies biological pathways and genes associated with variations in feed efficiency of growing pigs. *BMC Genomics* 18: 244, 2017. doi: 10.1186/s12864-017-3639-0.

13. **Le Naou T**, **Le Floc'h N**, **Louveau I**, **Gilbert H**, **Gondret F**. Metabolic changes and tissue responses to selection on residual feed intake in growing pigs. *J Anim Sci* 90: 4771–4780, 2012. doi: 10.2527/jas.2012-5226.

14. **Montagne L**, **Loisel F**, **Le Naou T**, **Gondret F**, **Gilbert H**, **Le Gall M**. Difference in short-term responses to a high-fiber diet in pigs divergently selected for residual feed intake1. *J Anim Sci* 92: 1512–1523, 2014. doi: 10.2527/jas.2013-6623.

15. **Aliakbari A**, **Zemb O**, **Billon Y**, **Barilly C**, **Ahn I**, **Riquet J**, **Gilbert H**. Genetic relationships between feed efficiency and gut microbiome in pig lines selected for residual feed intake. *J Anim Breed Genet* 138: 491–507, 2021. doi: 10.1111/jbg.12539.

16. **Meunier-Salaün MC**, **Guérin C**, **Billon Y**, **Sellier P**, **Noblet J**, **Gilbert H**. Divergent selection for residual feed intake in group-housed growing pigs: characteristics of physical and behavioural activity according to line and sex. *Animal* 8: 1898–1906, 2014. doi: 10.1017/S1751731114001839.

17. **Le Gall M**, **Thenet S**, **Aguanno D**, **Jarry A-C**, **Genser L**, **Ribeiro-Parenti L**, **Joly F**, **Ledoux S**, **Bado A**, **Le Beyec J**. Intestinal plasticity in response to nutrition and gastrointestinal surgery. *Nutr Rev* 77: 129–143, 2019. doi: 10.1093/nutrit/nuy064.

18. **Amin T**, **Mercer JG**. Hunger and Satiety Mechanisms and Their Potential Exploitation in the Regulation of Food Intake. *Curr Obes Rep* 5: 106–112, 2016. doi: 10.1007/s13679-015-0184-5.

19. **Suzuki K**, **Simpson KA**, **Minnion JS**, **Shillito JC**, **Bloom SR**. The role of gut hormones and the hypothalamus in appetite regulation. *Endocr J* 57: 359–372, 2010. doi: 10.1507/endocrj.K10E-077.

20. **Zhang H**, **Xia P**, **Feng L**, **Jia M**, **Su Y**. Feeding Frequency Modulates the Intestinal Transcriptome Without Affecting the Gut Microbiota in Pigs With the Same Daily Feed Intake. *Front Nutr* 8: 743343, 2021. doi: 10.3389/fnut.2021.743343.

21. **Mazurais D**, **Romé V**, **Cahu A**, **Gadie**, **Le Huërou-Luron I**. Fasting and refeeding impacts on piglet jejunal transcriptome during weaning period. *Livest Sci* 108: 13–16, 2007. doi: 10.1016/j.livsci.2007.01.006.

22. **Yoshioka M**, **Bolduc C**, **Raymond V**, **St-Amand J**. High-fat meal-induced changes in the duodenum mucosa transcriptome. *Obes Silver Spring Md* 16: 2302–2307, 2008. doi: 10.1038/oby.2008.352.

23. **Ma K**, **Hu Y**, **Smith DE**. Influence of fed-fasted state on intestinal PEPT1 expression and in vivo pharmacokinetics of glycylsarcosine in wild-type and Pept1 knockout mice. *Pharm Res* 29: 535–545, 2012. doi: 10.1007/s11095-011-0580-9.

24. **Hediger MA**, **Clémençon B**, **Burrier RE**, **Bruford EA**. The ABCs of membrane transporters in health and disease (SLC series): Introduction. *Mol Aspects Med* 34: 95–107, 2013. doi: 10.1016/j.mam.2012.12.009.

25. **Schumann T**, **König J**, **Henke C**, **Willmes DM**, **Bornstein SR**, **Jordan J**, **Fromm MF**, **Birkenfeld AL**. Solute Carrier Transporters as Potential Targets for the Treatment of Metabolic Disease. *Pharmacol Rev* 72: 343–379, 2020. doi: 10.1124/pr.118.015735.

26. **Zhang Y**, **Zhang Y**, **Sun K**, **Meng Z**, **Chen L**. The SLC transporter in nutrient and metabolic sensing, regulation, and drug development. *J Mol Cell Biol* 11: 1–13, 2019. doi: 10.1093/jmcb/mjy052.

27. **Bogdanović O**, **Lister R**. DNA methylation and the preservation of cell identity. *Curr Opin Genet Dev* 46: 9–14, 2017. doi: 10.1016/j.gde.2017.06.007.

28. **Mattei AL**, **Bailly N**, **Meissner A**. DNA methylation: a historical perspective. *Trends Genet* 38: 676–707, 2022. doi: 10.1016/j.tig.2022.03.010.

29. **Pinho RM**, **Maga EA**. DNA methylation as a regulator of intestinal gene expression. *Br J Nutr* 126: 1611–1625, 2021. doi: 10.1017/S0007114521000556.

30. **Deaton AM**, **Bird A**. CpG islands and the regulation of transcription. *Genes Dev* 25: 1010–1022, 2011. doi: 10.1101/gad.2037511.

31. **Sheaffer KL**, **Kim R**, **Aoki R**, **Elliott EN**, **Schug J**, **Burger L**, **Schübeler D**, **Kaestner KH**. DNA methylation is required for the control of stem cell differentiation in the small intestine. *Genes Dev* 28: 652–664, 2014. doi: 10.1101/gad.230318.113.

32. **Kaaij LTJ**, **van de Wetering M**, **Fang F**, **Decato B**, **Molaro A**, **van de Werken HJG**, **van Es JH**, **Schuijers J**, **de Wit E**, **de Laat W**, **Hannon GJ**, **Clevers HC**, **Smith AD**, **Ketting RF**. DNA methylation dynamics during intestinal stem cell differentiation reveals enhancers driving gene expression in the villus. *Genome Biol* 14: R50, 2013. doi: 10.1186/gb-2013-14-5-r50.

33. **Tao S**, **Zhou T**, **Saelao P**, **Wang Y**, **Zhu Y**, **Li T**, **Zhou H**, **Wang J**. Intrauterine Growth Restriction Alters the Genome-Wide DNA Methylation Profiles in Small Intestine, Liver and Longissimus Dorsi Muscle of Newborn Piglets. *Curr Protein Pept Sci* 20: 713–726, 2019. doi: 10.2174/1389203720666190124165243.

34. **Devos J**, **Behrouzi A**, **Paradis F**, **Straathof C**, **Li C**, **Colazo M**, **Block H**, **Fitzsimmons C**. Genetic potential for residual feed intake and diet fed during early- to mid-gestation influences post-natal DNA methylation of imprinted genes in muscle and liver tissues in beef cattle. *J Anim Sci* 99: skab140, 2021. doi: 10.1093/jas/skab140.

35. **Hjort L**, **Jørgensen SW**, **Gillberg L**, **Hall E**, **Brøns C**, **Frystyk J**, **Vaag AA**, **Ling C**. 36 h fasting of young men influences adipose tissue DNA methylation of LEP and ADIPOQ in a birth weight-dependent manner. *Clin Epigenetics* 9: 40, 2017. doi: 10.1186/s13148-017-0340-8.

36. **GenESI**. Pig Innovative Breeding Experimental Facility. .

37. **GET**. Genome & Transcriptome Facility. .

38. **Ewels PA**, **Peltzer A**, **Fillinger S**, **Patel H**, **Alneberg J**, **Wilm A**, **Garcia MU**, **Di Tommaso P**, **Nahnsen S**. The nf-core framework for community-curated bioinformatics pipelines. *Nat Biotechnol* 38: 276–278, 2020. doi: 10.1038/s41587-020-0439-x.

39. **Patro R**, **Duggal G**, **Love MI**, **Irizarry RA**, **Kingsford C**. Salmon provides fast and bias-aware quantification of transcript expression. *Nat Methods* 14: 417–419, 2017. doi: 10.1038/nmeth.4197.

40. **Cunningham F**, **Allen JE**, **Allen J**, **Alvarez-Jarreta J**, **Amode MR**, **Armean IM**, **Austine-Orimoloye O**, **Azov AG**, **Barnes I**, **Bennett R**, **Berry A**, **Bhai J**, **Bignell A**, **Billis K**, **Boddu S**, **Brooks L**, **Charkhchi M**, **Cummins C**, **Da Rin Fioretto L**, **Davidson C**, **Dodiya K**, **Donaldson S**, **El Houdaigui B**, **El Naboulsi T**, **Fatima R**, **Giron CG**, **Genez T**, **Martinez JG**, **Guijarro-Clarke C**, **Gymer A**, **Hardy M**, **Hollis Z**, **Hourlier T**, **Hunt T**, **Juettemann T**, **Kaikala V**, **Kay M**, **Lavidas I**, **Le T**, **Lemos D**, **Marugán JC**, **Mohanan S**, **Mushtaq A**, **Naven M**, **Ogeh DN**, **Parker A**, **Parton A**, **Perry M**, **Piližota I**, **Prosovetskaia I**, **Sakthivel MP**, **Salam AIA**, **Schmitt BM**, **Schuilenburg H**, **Sheppard D**, **Pérez-Silva JG**, **Stark W**, **Steed E**, **Sutinen K**, **Sukumaran R**, **Sumathipala D**, **Suner M-M**, **Szpak M**, **Thormann A**, **Tricomi FF**, **Urbina-Gómez D**, **Veidenberg A**, **Walsh TA**, **Walts B**, **Willhoft N**, **Winterbottom A**, **Wass E**, **Chakiachvili M**, **Flint B**, **Frankish A**, **Giorgetti S**, **Haggerty L**, **Hunt SE**, **IIsley GR**, **Loveland JE**, **Martin FJ**, **Moore B**, **Mudge JM**, **Muffato M**, **Perry E**, **Ruffier M**, **Tate J**, **Thybert D**, **Trevanion SJ**, **Dyer S**, **Harrison PW**, **Howe KL**, **Yates AD**, **Zerbino DR**, **Flicek P**. Ensembl 2022. *Nucleic Acids Res* 50: D988–D995, 2022. doi: 10.1093/nar/gkab1049.

41. **Soneson C**, **Love MI**, **Robinson MD**. Differential analyses for RNA-seq: transcript-level estimates improve gene-level inferences. *F1000Research* 4: 1521, 2015. doi: 10.12688/f1000research.7563.1.

42. **Law CW**, **Chen Y**, **Shi W**, **Smyth GK**. voom: precision weights unlock linear model analysis tools for RNA-seq read counts. *Genome Biol* 15: R29, 2014. doi: 10.1186/gb-2014-15-2-r29.

43. **Wu T**, **Hu E**, **Xu S**, **Chen M**, **Guo P**, **Dai Z**, **Feng T**, **Zhou L**, **Tang W**, **Zhan L**, **Fu X**, **Liu S**, **Bo X**, **Yu G**. clusterProfiler 4.0: A universal enrichment tool for interpreting omics data. *The Innovation* 2: 100141, 2021. doi: 10.1016/j.xinn.2021.100141.

44. **Gu Z**, **Eils R**, **Schlesner M**. Complex heatmaps reveal patterns and correlations in multidimensional genomic data. *Bioinformatics* 32: 2847–2849, 2016. doi: 10.1093/bioinformatics/btw313.

45. **Conway JR**, **Lex A**, **Gehlenborg N**. UpSetR: an R package for the visualization of intersecting sets and their properties. *Bioinformatics* 33: 2938–2940, 2017. doi: 10.1093/bioinformatics/btx364.

46. **Carbon, Seth**, **Mungall, Chris**. Gene Ontology Data Archive. Zenodo: 2023.

47. **The Gene Ontology Consortium**. The Gene Ontology Resource: 20 years and still GOing strong. *Nucleic Acids Res* 47: D330–D338, 2019. doi: 10.1093/nar/gky1055.

48. **Riebler A**, **Menigatti M**, **Song JZ**, **Statham AL**, **Stirzaker C**, **Mahmud N**, **Mein CA**, **Clark SJ**, **Robinson MD**. BayMeth: improved DNA methylation quantification for affinity capture sequencing data using a flexible Bayesian approach. *Genome Biol* 15: R35, 2014. doi: 10.1186/gb-2014-15-2-r35.

49. **Gord Brown <Gdbzork@Gmail.Com>**. GreyListChIP. Bioconductor: 2017.

50. **Gu Z**, **Eils R**, **Schlesner M**, **Ishaque N**. EnrichedHeatmap: an R/Bioconductor package for comprehensive visualization of genomic signal associations. *BMC Genomics* 19: 234, 2018. doi: 10.1186/s12864-018-4625-x.

51. **Love MI**, **Huber W**, **Anders S**. Moderated estimation of fold change and dispersion for RNA-seq data with DESeq2. *Genome Biol* 15: 550, 2014. doi: 10.1186/s13059-014-0550-8.

52. **Saci S**, **Devailly G**. epistack: An R package to visualise stack profiles of epigenomic signals [Online]. [date unknown]. https://bioconductor.org/packages/release/bioc/html/epistack.html.

53. **Stewart AK**, **Kurschat CE**, **Vaughan-Jones RD**, **Alper SL**. Putative Re-entrant Loop 1 of AE2 Transmembrane Domain Has a Major Role in Acute Regulation of Anion Exchange by pH. *J Biol Chem* 284: 6126–6139, 2009. doi: 10.1074/jbc.M802051200.

54. **Harris HA**, **Friedman C**, **Starling AP**, **Dabelea D**, **Johnson SL**, **Fuemmeler BF**, **Jima D**, **Murphy SK**, **Hoyo C**, **Jansen PW**, **Felix JF**, **Mulder R**. An epigenome-wide association study of child appetitive traits and DNA methylation. Genetics.

55. **Vancamelbeke M**, **Vermeire S**. The intestinal barrier: a fundamental role in health and disease. *Expert Rev Gastroenterol Hepatol* 11: 821–834, 2017. doi: 10.1080/17474124.2017.1343143.

56. **Gilbert H**, **Ruesche J**, **Muller N**, **Billon Y**, **Begos V**, **Montagne L**. Responses to weaning in two pig lines divergently selected for residual feed intake depending on diet1. *J Anim Sci* 97: 43–54, 2019. doi: 10.1093/jas/sky416.

57. **Montagne L**, **Gilbert H**, **Muller N**, **Le Floc'h N**. Physiological response to the weaning in two pig lines divergently selected for residual feed intake. *J Anim Physiol Anim Nutr* 106: 802–812, 2022. doi: 10.1111/jpn.13622.

58. **de Mendoza A**, **Nguyen TV**, **Ford E**, **Poppe D**, **Buckberry S**, **Pflueger J**, **Grimmer MR**, **Stolzenburg S**, **Bogdanovic O**, **Oshlack A**, **Farnham PJ**, **Blancafort P**, **Lister R**. Large-scale manipulation of promoter DNA methylation reveals context-specific transcriptional responses and stability. *Genome Biol* 23: 163, 2022. doi: 10.1186/s13059-022-02728-5.

59. **Aliakbari A**, **Delpuech E**, **Labrune Y**, **Riquet J**, **Gilbert H**. The impact of training on data from genetically-related lines on the accuracy of genomic predictions for feed efficiency traits in pigs. *Genet Sel Evol* 52: 57, 2020. doi: 10.1186/s12711-020-00576-0.

60. **Jones PA**, **Liang G**. Rethinking how DNA methylation patterns are maintained. *Nat Rev Genet* 10: 805–811, 2009. doi: 10.1038/nrg2651.

61. **Aguet F**, **Alasoo K**, **Li YI**, **Battle A**, **Im HK**, **Montgomery SB**, **Lappalainen T**. Molecular quantitative trait loci. *Nat Rev Methods Primer* 3: 4, 2023. doi: 10.1038/s43586-022-00188-6.

62. **Nguyen NTT**, **Vincens P**, **Dufayard JF**, **Roest Crollius H**, **Louis A**. Genomicus in 2022: comparative tools for thousands of genomes and reconstructed ancestors. *Nucleic Acids Res* 50: D1025–D1031, 2022. doi: 10.1093/nar/gkab1091.

63. **Heinritz SN**, **Mosenthin R**, **Weiss E**. Use of pigs as a potential model for research into dietary modulation of the human gut microbiota. *Nutr Res Rev* 26: 191–209, 2013. doi: 10.1017/S0954422413000152.

64. **Lunney JK**, **Van Goor A**, **Walker KE**, **Hailstock T**, **Franklin J**, **Dai C**. Importance of the pig as a human biomedical model. *Sci Transl Med* 13: eabd5758, 2021. doi: 10.1126/scitranslmed.abd5758.

65. **Zhang Q**, **Widmer G**, **Tzipori S**. A pig model of the human gastrointestinal tract. *Gut Microbes* 4: 193–200, 2013. doi: 10.4161/gmic.23867.

66. **GenoToul Bioinfo**. GenoToul Bioinformatics Facility.

FIGURE LEGENDS

Figure 1: Experimental setup. **A.** 24 pigs from two pig lines (12 LRFI and 12 HRFI) were used, distributed in 3 litters of 4 pigs for each line, with two males and two females in each litter (to the exception of litter E). Half of the pigs were fasted while the other half was fed before sampling. **B.** Fasting procedure. Pigs were slotted into two pens with ad libitum feeding. Feed was removed from the two pens overnight, and reintroduced in the morning into one of the pens 2 hours before sampling started in this pen.

Figure 2: Differential gene expression between the duodenum of LRFI and HRFI lines. **A.** 1,106 genes were detected differentially expressed between LRFI and HRFI, including 464 genes upregulated in LRFI

(top) and 642 genes upregulated on the HRFI line (bottom). Samples from fasted and fed pigs were analyzed together for each line. **B & C.** Gene Ontology - Biological Process (GO-BP) enrichment analysis. GO-BP terms statistically enriched in the 642 genes upregulated on the HRFI line (**B**) and the 464 genes upregulated in LRFI line (**C**) are displayed as a tree using Jaccard similarity between each pair of GO-BP.

Figure 3: Duodenum transcriptomic response to feed intake. **A.** Gene expression heatmap of the 2,225 genes differentially expressed by feed intake in LRFI (2,222 genes), in HRFI (61 genes, including 58 genes also affected by feed intake in LRFI). **B.** Upset diagram showing the overlap between differentially expressed gene lists, between LRFI and HRFI (green), and due to feed intake in LRFI pigs (blue) or HRFI pigs (red). **C, D & E.** Gene Ontology - Biological Process (GO-BP) enrichment analysis. GO-BP terms statistically enriched in the 1,050 genes upregulated upon fasting in the LRFI line (**C**), the 1,172 genes upregulated in fed pigs from the LRFI line (**D**), and the 41 genes upregulated in fed pigs from the HRFI line (**E**) are displayed as a tree using Jaccard similarity between each pair of GO-BP. **F.** Gene expression heatmap of the 185 genes differentially expressed both by line and by feed intake in LRFI and/or HRFI pigs.

Figure 4: Gene expression heatmaps of the 59 SLC genes (**A**) or 18 tight junction genes (**B**) that are differentially expressed either between the LRFI and HRFI lines, or by feed intake in each line. Transporter names and known substrates are noted on the right of the heatmap. Three symbolic columns indicate if each gene is significantly differentially expressed (marked with "*") or not (marked with "·") between the two lines (Line column), or by feed intake in the LRFI line (LRFI column), or by feed intake in the HRFI line (HRFI column). Side trees are coloured according to hierarchical clustering, and are only used as visualisation guides.

Figure 5: Differentially methylated regions in the duodenum between LRFI and HRFI samples. **A.** Upset plot of differentially methylated regions. Green: between LRFI and HRFI samples. Blue: between fasted and fed samples in LRFI pigs. Red: between fasted and fed samples in HRFI pigs **B.** DNA methylation stack profiles at differentially methylated regions between LRFI and HRFI samples. Top: log2 Fold Change (FC) of MeDP-seq normalised coverage at DMR. The 409 LRFI/HRFI DMRs are sorted according to their fold change. Then: each DMR is categorised into a hypermethylated in LRFI bin (hyperM, red) or hypomethyated in LRFI bin (hypoM, blue). Then: Average DNA methylation ratio at ± 2.5kb of DMR centers, in LRFI (blue) or HRFI (red) samples. Bottom: Distribution of fold changes in each bin, then average DNA methylation ratios in each bin (hyperM in LRFI: red, hypoM in LRFI: blue).

Figure 6: Some differentially methylated regions at proximity differentially expressed genes. **A,C, E, G, I, K:** DNA methylation profiles around differentially methylated regions. From top to bottom: gene structure in black. Thick boxes are exons, thin lines are introns, arrows indicate gene direction. Grey box indicates DMR location. Then, average DNA methylation ratio profiles ± 95% confidence interval per line (**A, C, E, G, I,** blue: LRFI, red: HRFI) or per condition in each line (**K**, light blue: LRFI fasted, dark blue: LRFI fed, light red: HRFI fasted, dark red: HRFI fed). Then genome coordinates of the corresponding region. B, **D, F, H, J, L:** Gene expression values in LRFI fasted (light blue), LRFI fed (dark blue), HRFI fasted (light red), HRFI fed (dark red) samples. Unit in transcript per million (TPM). Each dot is a sample, and boxplots are added to ease visualisation. NS: non significant. *: FDR-adjusted p-values < 0.05. **: FDR-adjusted p-values < 0.01. Adjusted p-values are from the differential expression analysis using limma voom.

Large-white pig population

Divergent selection on feed efficiency for 10 generations

Fed vs overnight-fasted pigs

Duodenum mucosa dissection

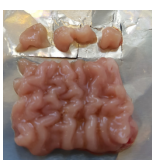

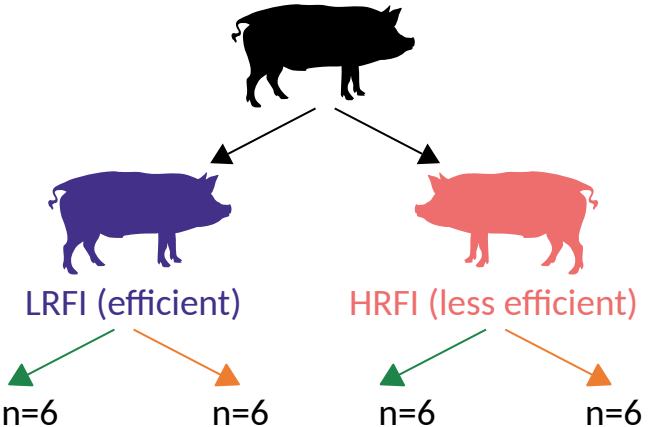

Gene expression differences	LRFI	LRFI vs HRFI	HRFI
LRFI vs HRFI		++	
Fed vs fasted	+++		+

DNA methylation differences			
LRFI vs HRFI		+	
Fed vs fasted	+/-		-

A

Line

LRFI HRFI

Family

A B C D E F

Sex

F M

Condition

fasted fed

B

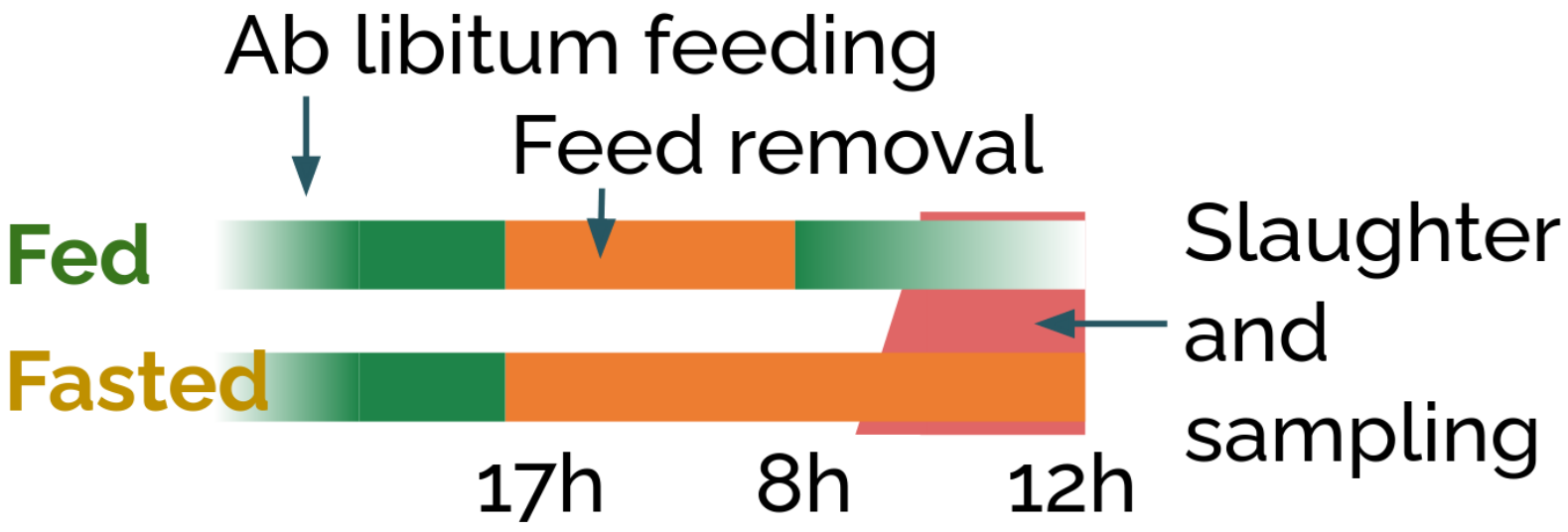

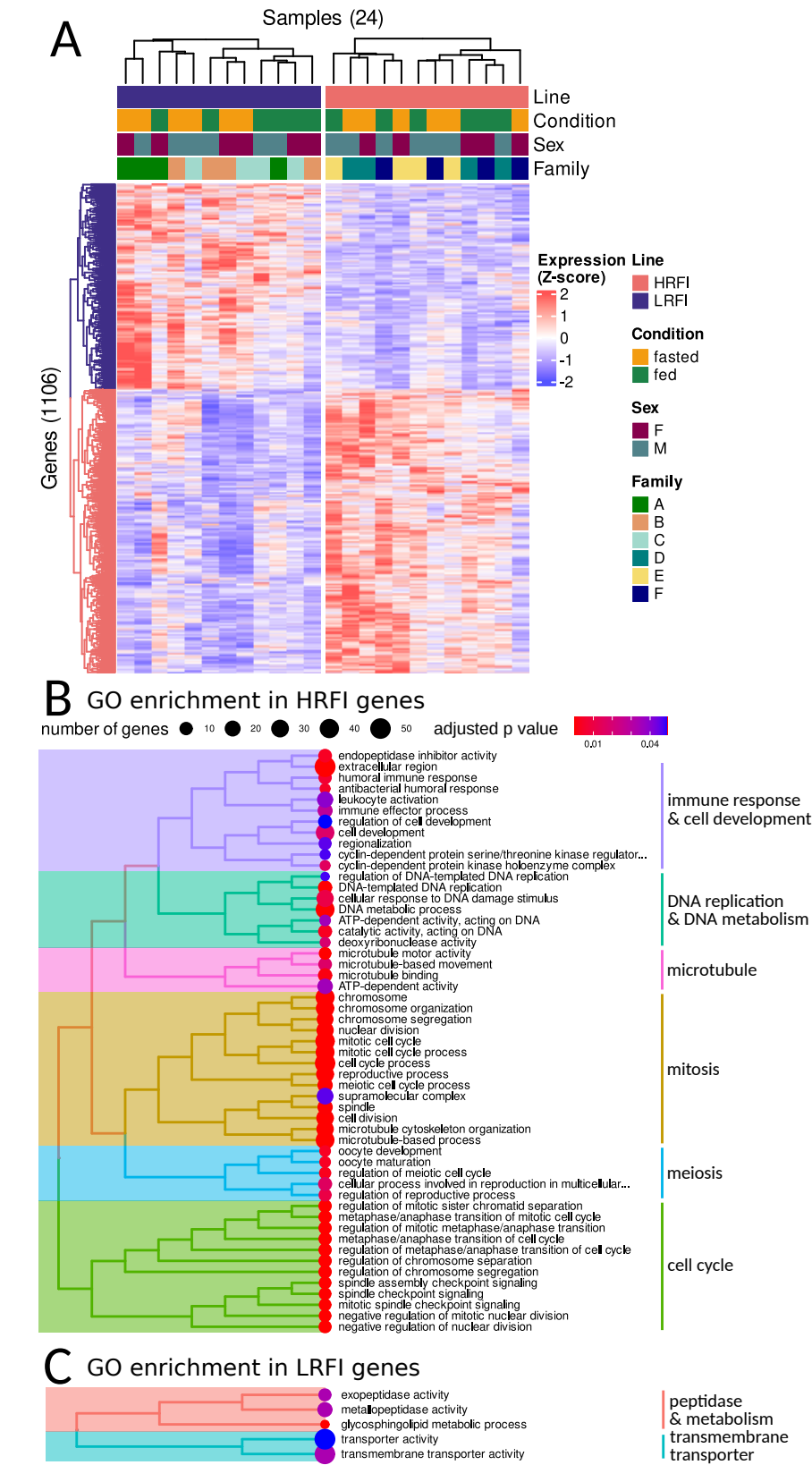
A
Samples (24)
Line
Condition
Sex
Family
Genes (1106)
Expression (Z-score)
2
1
0
-1
-2
Line
HRFI
LRFI
Condition
fasted
fed
Sex
F
M
Family
A
B
C
D
E
F
B
GO enrichment in HRFI genes
number of genes
10
20
30
40
50
adjusted p value
0.01
0.04
endopeptidase inhibitor activity
extracellular region
humoral immune response
antibacterial humoral response
leukocyte activation
immune effector process
regulation of cell development
cell development
regionalization
cyclin-dependent protein serine/threonine kinase regulator...
cyclin-dependent protein kinase holoenzyme complex
regulation of DNA-templated DNA replication
DNA-templated DNA replication
cellular response to DNA damage stimulus
DNA metabolic process
ATP-dependent activity, acting on DNA
catalytic activity, acting on DNA
deoxyribonuclease activity
microtubule motor activity
microtubule-based movement
microtubule binding
ATP-dependent activity
chromosome
chromosome organization
chromosome segregation
nuclear division
mitotic cell cycle
mitotic cell cycle process
cell cycle process
reproductive process
meiotic cell cycle process
supramolecular complex
spindle
cell division
microtubule cytoskeleton organization
microtubule-based process
oocyte development
oocyte maturation
regulation of meiotic cell cycle
cellular process involved in reproduction in multicellular...
regulation of reproductive process
regulation of mitotic sister chromatid separation
metaphase/anaphase transition of mitotic cell cycle
regulation of mitotic metaphase/anaphase transition
metaphase/anaphase transition of cell cycle
regulation of metaphase/anaphase transition of cell cycle
regulation of chromosome separation
regulation of chromosome segregation
spindle assembly checkpoint signaling
spindle checkpoint signaling
mitotic spindle checkpoint signaling
negative regulation of mitotic nuclear division
negative regulation of nuclear division
immune response & cell development
DNA replication & DNA metabolism
microtubule
mitosis
meiosis
cell cycle
C
GO enrichment in LRFI genes
exopeptidase activity
metallopeptidase activity
glycosphingolipid metabolic process
transporter activity
transmembrane transporter activity
peptidase & metabolism
transmembrane transporter

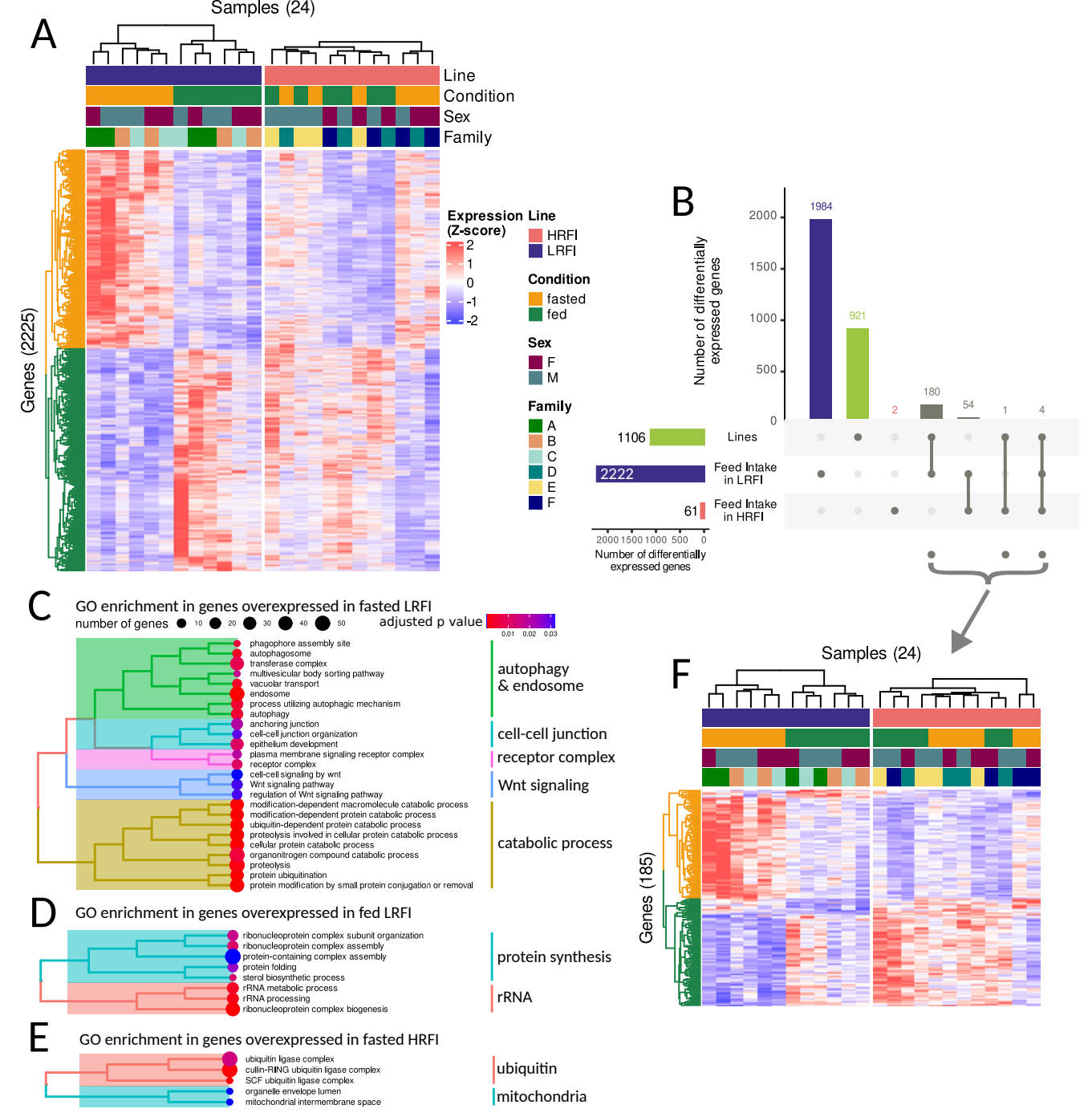
A
Samples (24)
Line
Condition
Sex
Family
Genes (2225)
Expression (Z-score)
2
1
0
-1
-2
Line
HRFI
LRFI
Condition
fasted
fed
Sex
F
M
Family
A
B
C
D
E
F
B
Number of differentially expressed genes
2000
1500
1000
500
0
1984
921
2
180
54
1
4
1106
2222
61
Lines
Feed Intake in LRFI
Feed Intake in HRFI
2000 1500 1000 500 0
Number of differentially expressed genes
C
GO enrichment in genes overexpressed in fasted LRFI
number of genes
10
20
30
40
50
adjusted p value
0.01
0.02
0.03
phagophore assembly site
autophagosome
transferase complex
multivesicular body sorting pathway
vacuolar transport
endosome
process utilizing autophagic mechanism
autophagy
anchoring junction
cell-cell junction organization
epithelium development
plasma membrane signaling receptor complex
receptor complex
cell-cell signaling by wnt
Wnt signaling pathway
regulation of Wnt signaling pathway
modification-dependent macromolecule catabolic process
modification-dependent protein catabolic process
ubiquitin-dependent protein catabolic process
proteolysis involved in cellular protein catabolic process
cellular protein catabolic process
organonitrogen compound catabolic process
proteolysis
protein ubiquitination
protein modification by small protein conjugation or removal
autophagy & endosome
cell-cell junction
receptor complex
Wnt signaling
catabolic process
D
GO enrichment in genes overexpressed in fed LRFI
ribonucleoprotein complex subunit organization
ribonucleoprotein complex assembly
protein-containing complex assembly
protein folding
sterol biosynthetic process
rRNA metabolic process
rRNA processing
ribonucleoprotein complex biogenesis
protein synthesis
rRNA
E
GO enrichment in genes overexpressed in fasted HRFI
ubiquitin ligase complex
cullin-RING ubiquitin ligase complex
SCF ubiquitin ligase complex
organelle envelope lumen
mitochondrial intermembrane space
ubiquitin
mitochondria
F
Samples (24)
Genes (185)

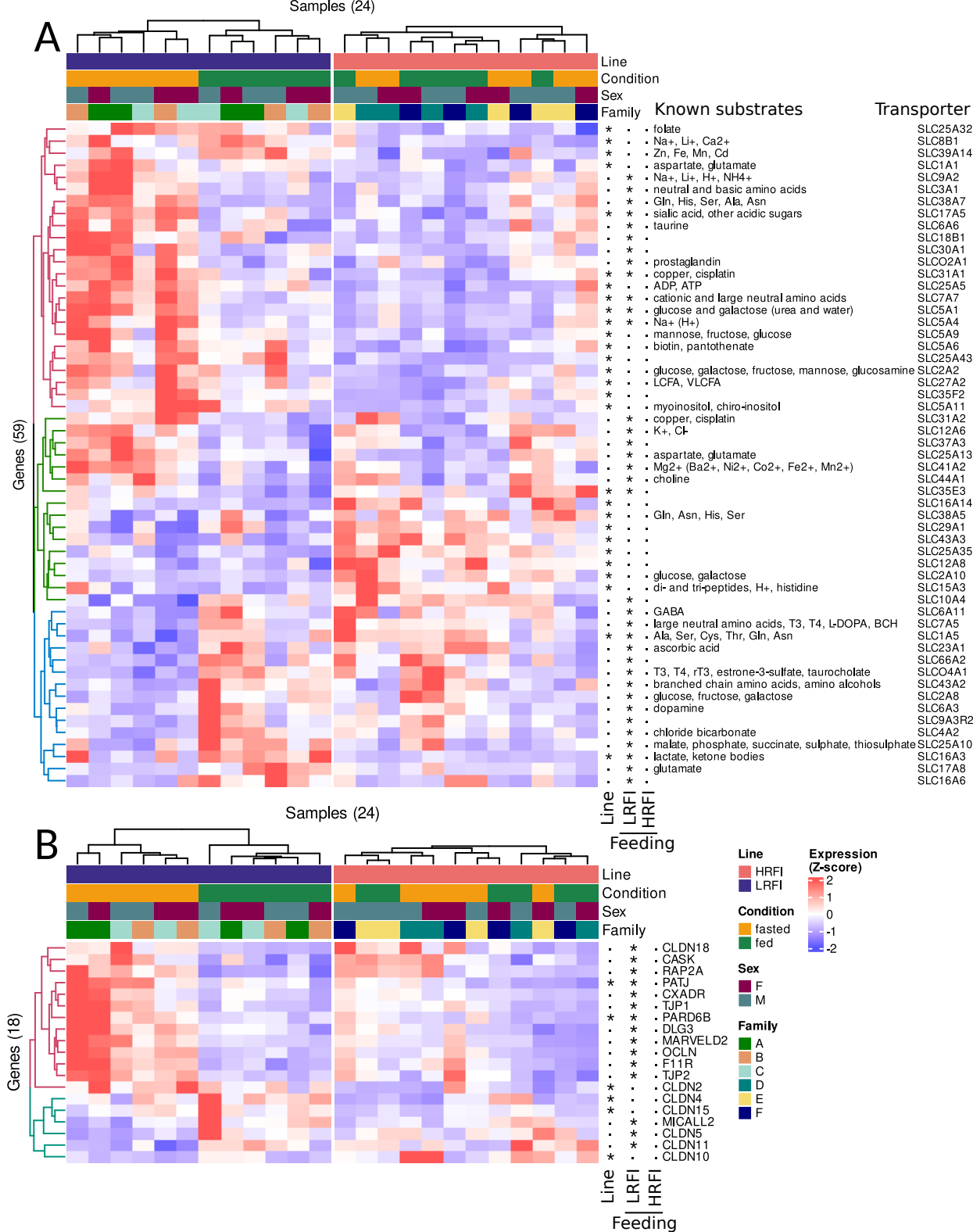
A
Samples (24)
Line
Condition
Sex
Family
Known substrates
Transporter
folate SLC25A32
Na+, Li+, Ca2+ SLC8B1
Zn, Fe, Mn, Cd SLC39A14
aspartate, glutamate SLC1A1
Na+, Li+, H+, NH4+ SLC9A2
neutral and basic amino acids SLC3A1
Gln, His, Ser, Ala, Asn SLC38A7
sialic acid, other acidic sugars SLC17A5
taurine SLC6A6
SLC18B1
SLC30A1
prostaglandin SLCO2A1
copper, cisplatin SLC31A1
ADP, ATP SLC25A5
cationic and large neutral amino acids SLC7A7
glucose and galactose (urea and water) SLC5A1
Na+ (H+) SLC5A4
mannose, fructose, glucose SLC5A9
biotin, pantothenate SLC5A6
SLC25A43
glucose, galactose, fructose, mannose, glucosamine SLC2A2
LCFA, VLCFA SLC27A2
SLC35F2
myoinositol, chiro-inositol SLC5A11
copper, cisplatin SLC31A2
K+, Cl- SLC12A6
SLC37A3
aspartate, glutamate SLC25A13
Mg2+ (Ba2+, Ni2+, Co2+, Fe2+, Mn2+) SLC41A2
choline SLC44A1
SLC35E3
SLC16A14
Gln, Asn, His, Ser SLC38A5
SLC29A1
SLC43A3
SLC25A35
SLC12A8
glucose, galactose SLC2A10
di- and tri-peptides, H+, histidine SLC15A3
SLC10A4
GABA SLC6A11
large neutral amino acids, T3, T4, L-DOPA, BCH SLC7A5
Ala, Ser, Cys, Thr, Gln, Asn SLC1A5
ascorbic acid SLC23A1
SLC66A2
T3, T4, rT3, estrone-3-sulfate, taurocholate SLCO4A1
branched chain amino acids, amino alcohols SLC43A2
glucose, fructose, galactose SLC2A8
dopamine SLC6A3
SLC9A3R2
chloride bicarbonate SLC4A2
malate, phosphate, succinate, sulphate, thiosulphate SLC25A10
lactate, ketone bodies SLC16A3
glutamate SLC17A8
SLC16A6
Genes (59)
Line
LRFI
HRFI
Feeding
Samples (24)
B
Line
Condition
Sex
Family
CLDN18
CASK
RAP2A
PATJ
CXADR
TJP1
PARD6B
DLG3
MARVELD2
OCLN
F11R
TJP2
CLDN2
CLDN4
CLDN15
MICALL2
CLDN5
CLDN11
CLDN10
Genes (18)
Line
LRFI
HRFI
Feeding
Line
HRFI
LRFI
Condition
fasted
fed
Sex
F
M
Family
A
B
C
D
E
F
Expression (Z-score)
2
1
0
-1
-2

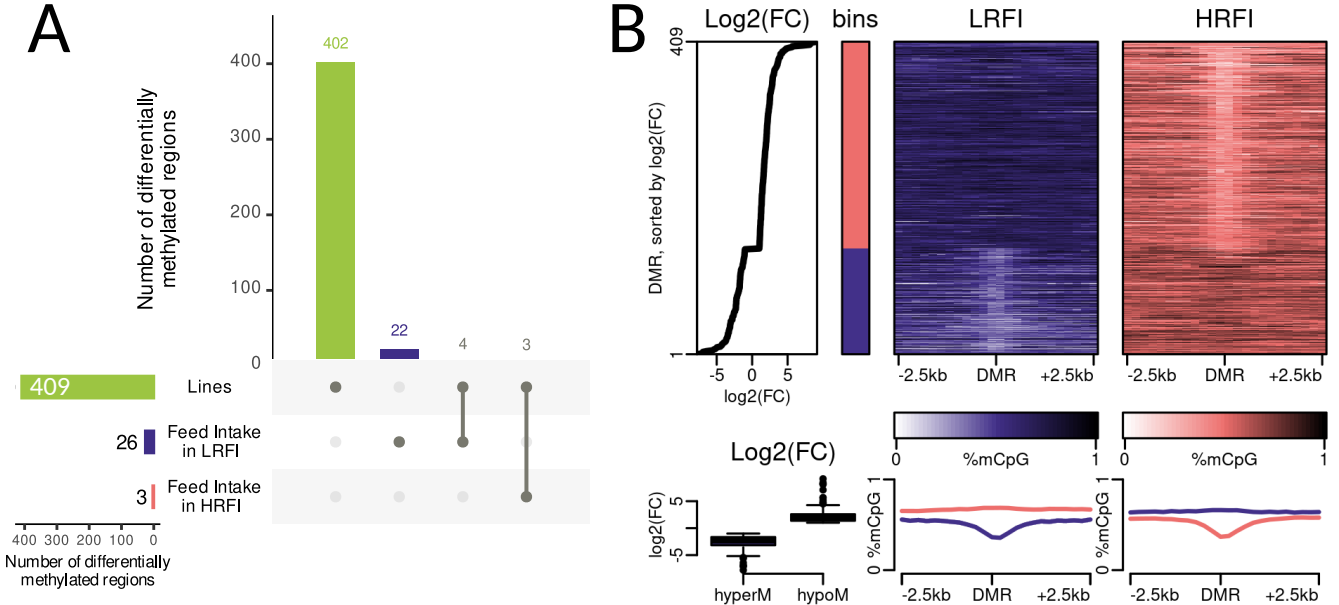
A
Number of differentially methylated regions
402
22
4
3
409
Lines
26
Feed Intake in LRFI
3
Feed Intake in HRFI
Number of differentially methylated regions
B
Log2(FC)
bins
LRFI
HRFI
DMR, sorted by log2(FC)
log2(FC)
-2.5kb
DMR
+2.5kb
%mCpG
hyperM
hypoM

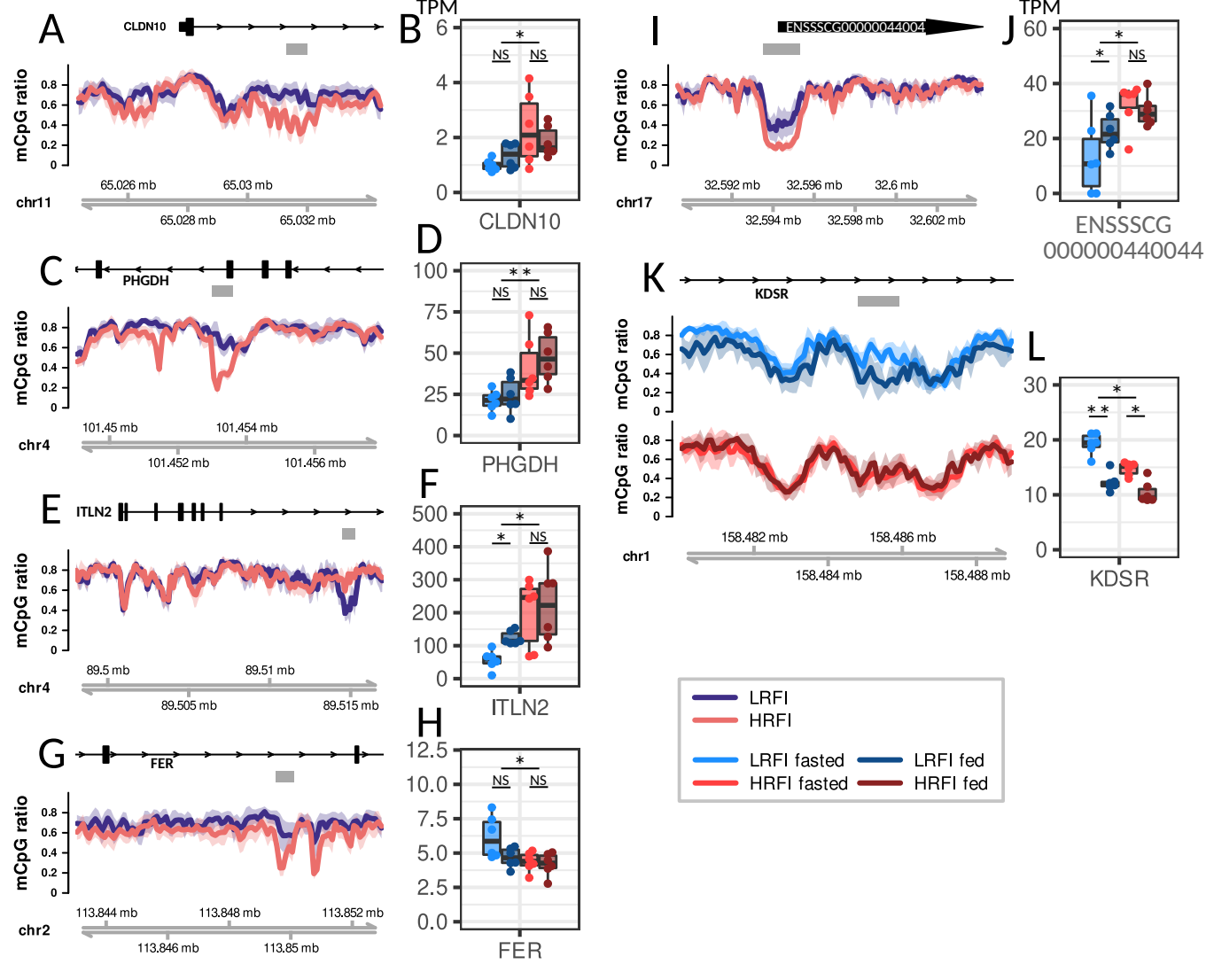
A
CLDN10
mCpG ratio
0.8
0.6
0.4
0.2
0
65.026 mb
65.03 mb
chr11
65.028 mb
65.032 mb
B
TPM
6
4
2
0
*
NS
NS
CLDN10
C
PHGDH
mCpG ratio
101.45 mb
101.454 mb
chr4
101.452 mb
101.456 mb
D
100
75
50
25
0
**
NS
NS
PHGDH
E
ITLN2
mCpG ratio
89.5 mb
89.51 mb
chr4
89.505 mb
89.515 mb
F
500
400
300
200
100
0
*
*
NS
ITLN2
G
FER
mCpG ratio
113.844 mb
113.848 mb
113.852 mb
chr2
113.846 mb
113.85 mb
H
12.5
10.0
7.5
5.0
2.5
0.0
*
NS
NS
FER
I
ENSSSCG00000044004
mCpG ratio
32.592 mb
32.596 mb
32.6 mb
chr17
32.594 mb
32.598 mb
32.602 mb
J
TPM
60
40
20
0
*
*
NS
ENSSSCG
000000440044
K
KDSR
mCpG ratio
158.482 mb
158.486 mb
chr1
158.484 mb
158.488 mb
L
30
20
10
0
*
**
*
KDSR
LRFI
HRFI
LRFI fasted
HRFI fasted
LRFI fed
HRFI fed